Second-harmonic Generation Microscopy of Tooth

Fu-Jen Kao*[a,b], Yung-Shun Wang[a], Mao-Kuo Huang[a], Sheng-Lung Huang[c], Ping-Chin Cheng[d]

[a]Department of Physics, National Sun Yat-sen University, Kaohsiung 80424, Taiwan, ROC
[b]Center for Neuroscience, National Sun Yat-sen University, Kaohsiung 80424, Taiwan, ROC
[c]Institute of Electro-Optical Engineering, National Sun Yat-sen University, Kaohsiung 80424, Taiwan, ROC
[d]Department of Electrical Engineering, University at Buffalo, Buffalo, NY 14260, USA

ABSTRACT

In this study, we have developed a high performance microscopic system to perform second-harmonic (SH) imaging on a tooth. The high sensitivity of the system allows acquisition rate of 300 seconds/frame with resolution at 512x512 pixels. The surface SH signal generated from the tooth is also carefully verified through micro-spectroscopy, polarization rotation, and wavelength tuning. In this way, we can ensure the authenticity of the signal. The enamel that encapsulates the dentine is known to possess highly ordered structures. The anisotropy of the structure is revealed in the microscopic SH images of the tooth sample.

Keywords: Second-harmonic generation, confocal microscopy, micro-spectroscopy, tooth, enamel

1. INTRODUCTION

Second-harmonic generation (SHG) is a highly coherent nonlinear optical process. It is often used in extending coherent light sources to shorter wavelengths[1] and to probe anisotropy of various structures in a specimen.[2,3] In combination with scanning optical microscopy, SHG can be used to image samples of highly ordered structure without resorting to dyes. Microscopic imaging employing SHG was first reported by Gannaway and Sheppard[4] in 1978. SHG mapping of nonlinear crystals, tissues, and polycrystalline molecular films has been reported.[5-8] However, the nonlinear susceptibility of different materials varies a lot. SHG signal from nonlinear crystals or crystalline structures is relatively strong and easy to detect. Whereas SHG from less ordered structure is much weaker and requires very sensitive detecting scheme for image mapping. In this study, we have employed a confocal microscope, a mode-locked Ti:sapphire laser, and a liquid-nitrogen-cooled back-illuminated CCD camera to form a very sensitive SHG scanning microscopic imaging system. The peak light intensity at the focal point is estimated to be greater than $1x10^{10}$ W/cm^2. At this intensity, generation of surface SHG is feasible.

The second-harmonic signal exhibits the characteristic square power dependence on incident power. However, the cross section for generating second-harmonic signal is very small. Given the high instantaneous intensity of the pumping beam, it is likely that other nonlinear processes may also take place, such as two-photon fluorescence[9], which also possesses square dependence on incident power. It is thus necessary to verify the measured signal to ensure the authenticity of image contrast as a result of SHG. We have employed the following techniques in the verification of measured signals, which include micro-spectroscopy, polarization rotation, and wavelength tuning.

2. EXPERIMENTAL SETUP

2.1 Scanning Confocal Microscope for SHG image acquisition

A mode-locked Ti:sapphire laser (Tsunami, Spectra-Physics) pumped by a frequency-doubled all-solid-state laser (Verdi, Coherent) provides ultrafast laser pulses centered at 780 nm with pulse width approximately 100 femtoseconds. The repetition rate of the laser is 82 MHz. For the acquisition of SHG microscopic images, a beam scanning confocal microscope (Fluoview, Olympus) and a liquid nitrogen cooled CCD camera with a back-illuminated chip of 512x512 pixels (Orbis II, SpectraSource) are carefully integrated as shown in Fig. 1. The galvo-mirror set of the confocal microscope scans the laser beam over a designated area of the sample. A dichroic mirror reflects the scanned images toward the CCD. A relay lens is used to image this scanned area to the CCD chip. In between the dichroic and the CCD imaging chip, band pass and interference filters are used to ensure that only the SH signal is passed.

*correspondence: Email:fjk@mail.nsysu.edu.tw; Telephone:+886-7-5253720; Fax: +886-7-5253709

In *Optical Sensing, Imaging, and Manipulation for Biological and Biomedical Applications*, Robert R. Alfano, Ping-Pei Ho, Arthur E. T. Chiou, Editors, Proceedings of SPIE Vol. 4082 (2000) • 0277-786X/00/$15.00

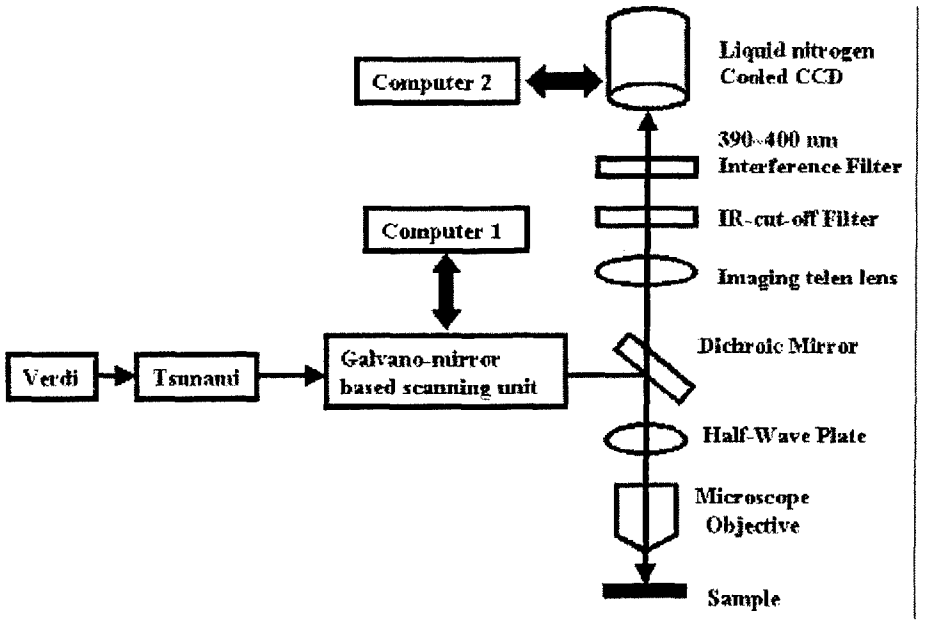

Figure 1. Schematics of the scanning microscope for SHG imaging. The mode-locked ti:sapphire laser provides ultrashort laser pulses for SHG excitation. The scanned area on the sample is imaged to the cooled CCD camera. The combination of IR cut-off filter and interference filter are used to reject non-SHG signal.

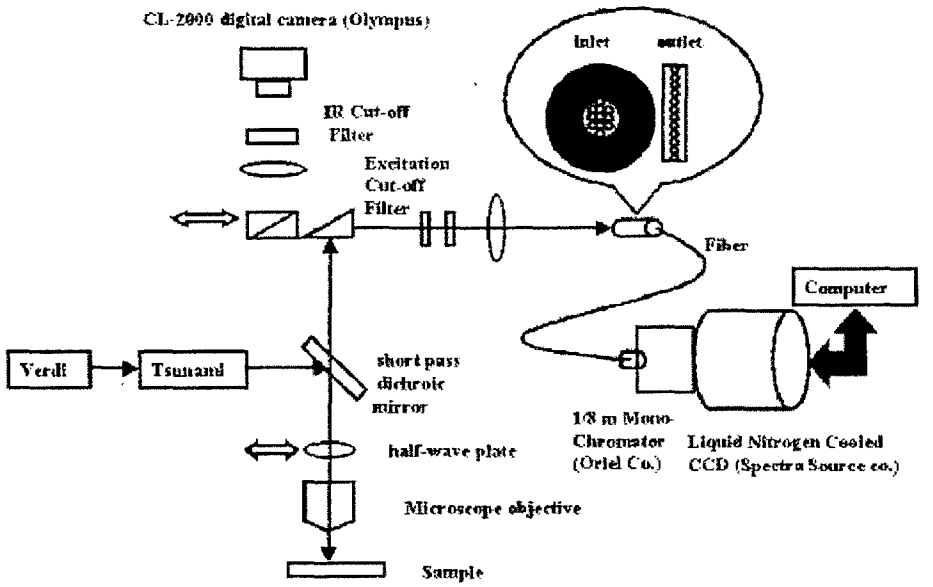

Figure 2. Schematic of the micro-spectroscopy. A specialized fiber bundle as shown in the figure is used to effectively couple the fluorescence collected from the microscope to the spectrometer. The outlet of the fiber bundle is vertically aligned to form a slit. The spectra acquired would form a band-like image on the CCD. The spectral range covered in a single frame depends on the grating installed in the monochromater. With a 600-groove grating, a spectral range of 150 nm can be contained in an image frame.

Using cooled CCD camera to integrate the very weak SHG signal is necessary, since the photomultiplier tubes that come with the confocal microscope are not sensitive enough.For a photo-multiplier to work, one would have to resort to pulse counting to integrate the signal and to reach sufficient signal-to-noise ratio. Pulse counting would nonetheless greatly

complicate the setup and subject the system to greater electronic noise. The use of a liquid nitrogen cooled CCD camera is very effective in this setup. Its very high quantum efficiency and natural ability to integrate signal enable efficient acquisition of SH images.

2.2 Micro-spectroscopy

A micro-spectroscopic setup is also employed to verify the nature of the signal thus obtained, as shown in Fig. 2. The laser beam is coupled into a modified fluorescence microscope (BX50, Olympus) through a dichroic mirror. The optical signal reflected from the sample is then guided to the spectrometer (77250, Oriel) through fiber coupling. The same liquid nitrogen cooled CCD camera described above is attached to the spectrometer for spectrum acquisition. Normally, a 10X objective of NA0.25 is employed for beam focusing. After loss in the optical path, a maximum power of 200mW is measured under the objective, which would correspond to intensity as high as $10^{10} W/cm^2$. Neutral density filters are used for power level adjustment. A half-wave plate is placed right next to the focusing objective. The half-wave plate is used to rotate the polarization of the incident beam so that the anisotropy of the sample can be detected.

The effectiveness of the above setup is tested with an unpolished KTP crystal. A fall-out primary tooth from a six year-old girl is used as the sample.

3. RESULTS

For SHG in the reflected direction, the intensity can be expressed as

$$I(2\omega) = \frac{32\pi^3\omega^2 \sec^2\theta_{2\omega}}{c^3 \varepsilon_1(\omega)\varepsilon_1^{\frac{1}{2}}(2\omega)} \left| e_{2\omega} \cdot \chi^{(2)} : e_\omega e_\omega \right|^2 I^2(\omega) \qquad (1)$$

According to the above equation, it is estimated that assuming $\left|\chi^{(2)}\right| \sim 10^{-15}$ esu, a SH output of 10^5 photons/second can be obtained. With a liquid nitrogen cooled CCD camera, such signal is readily detectable and is able to form clear images. The contribution to SHG contains both the surface layer and the bulk. The bulk contribution comes essentially from a layer of $\lambda/2\pi$ thick near the surface. It has been pointed out that if the structure of surface $\chi^{(2)}$ is sufficiently different from that of volume $\chi^{(2)}$, the relative intensity of $\chi^{(2)}_{surf}$ can be enhanced by polarization selection.

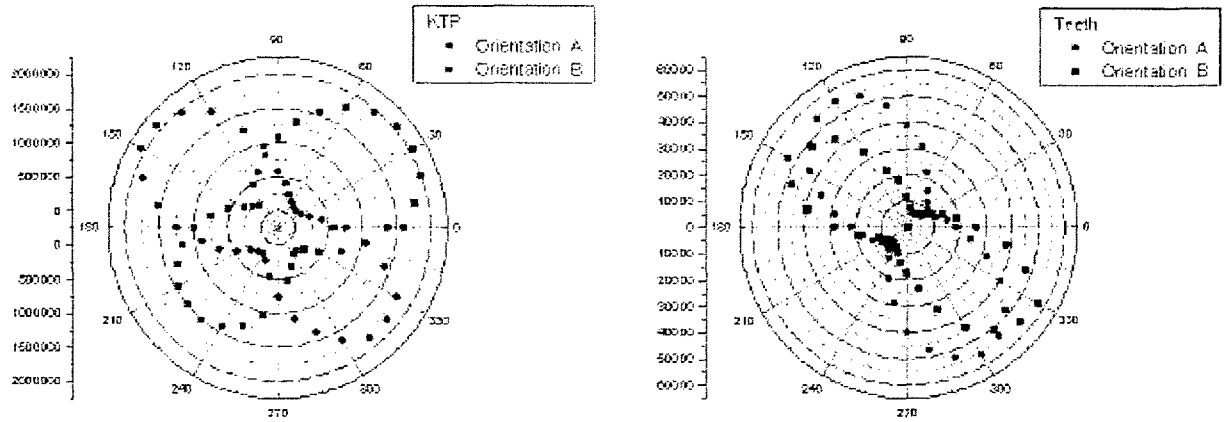

(a) (b)

Figure 3. Polar plots of SHG intensity as a function of polarization orientation from (a) a KTP crystal and (b) the primary tooth sample, respectively. The orientation of the samples is rotated to ensure that the anisotropy of the SHG distribution is resulted from the samples instead of the optical elements within the imaging microscope.

The surface SHG signal is usually very weak. It is thus necessary to discriminate the signal against other nonlinear backgrounds, such as two-photon fluorescence that has much higher cross section. In our measurements, methods of micro-spectroscopy and polarization rotation were employed to ensure the authenticity of the signal. Figure 3 shows the polar dependence of SHG intensity on incident beam polarization. The polarization of the incident beam is selected by the half-

wave plate placed next to the imaging objective. The dumb-bell shape of the plots clearly indicates the anisotropy of the sample.

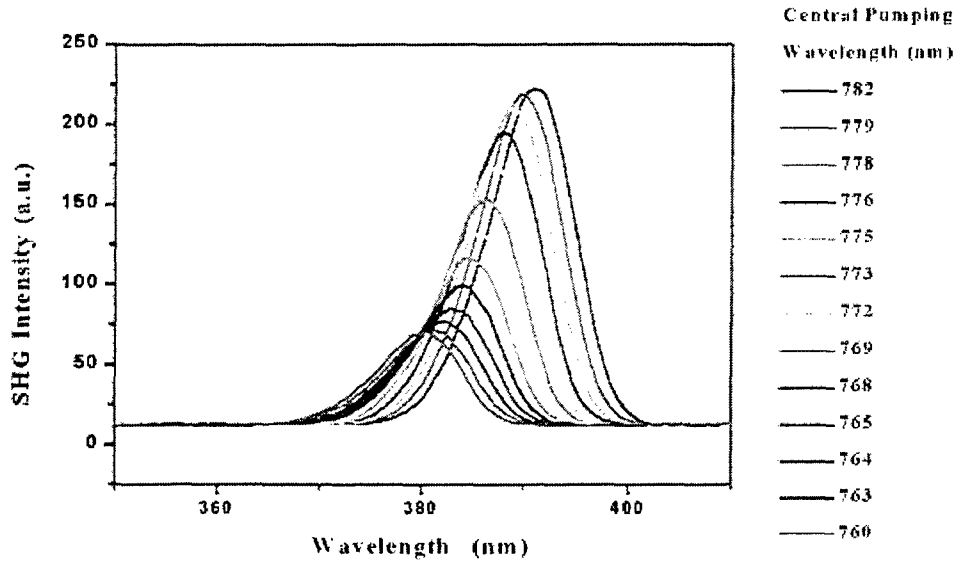

Figure 4. SHG Spectra as a function of pumping wavelength. The peak position of the detected spectra shifts accordingly as the wavelength of the excitation beam changes, clearly indicating the signal being SHG. The intensity of the SHG decreases as the central wavelength becomes shorter. This decrement reflects that the laser cavity is optimized to operate around 780 nm.

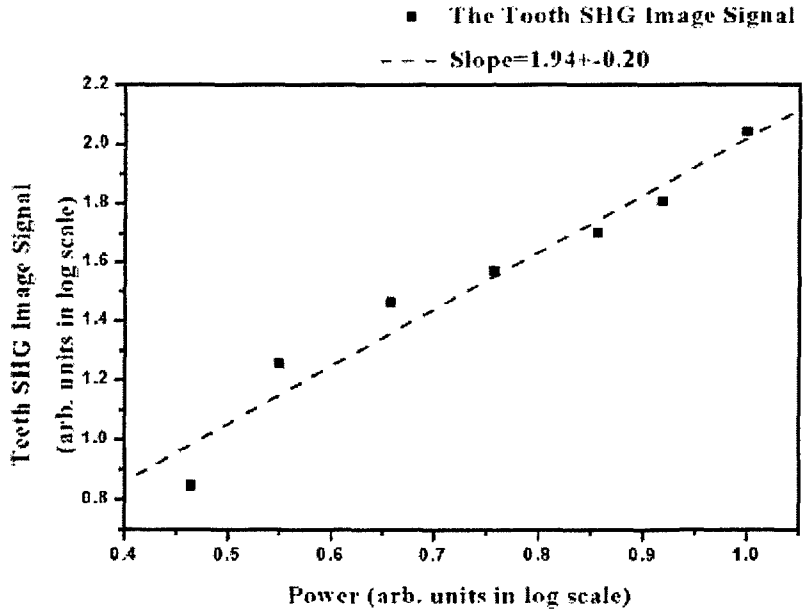

Figure 5. The SHG signal from the tooth as a function of incident power. The slope of 1.94 indicates the square power dependence of SHG.

Signal verification through micro-spectroscopy is shown in Fig. 4, where the SHG spectra as a function of pumping beam wavelength are plotted. The peak wavelength of the SHG shifts accordingly as the central wavelength of the pumping beam

is adjusted. This correlation in wavelength tuning strongly suggests that the signal is indeed SHG. In addition, the SHG signal as a function of incident power is shown in Fig. 5. The square power dependence indicates the two-photon nature of the excitation process. The microscopic reflection and SH images are shown in Fig. 6. The reflective images shown are somewhat obscured by scattering resulted from surface roughness and back-reflection from lens within the microscope system. The contrast from reflective images is not sensitive to polarization orientation. For comparison, the SHG images exhibit clear contrast and structural anisotropy.

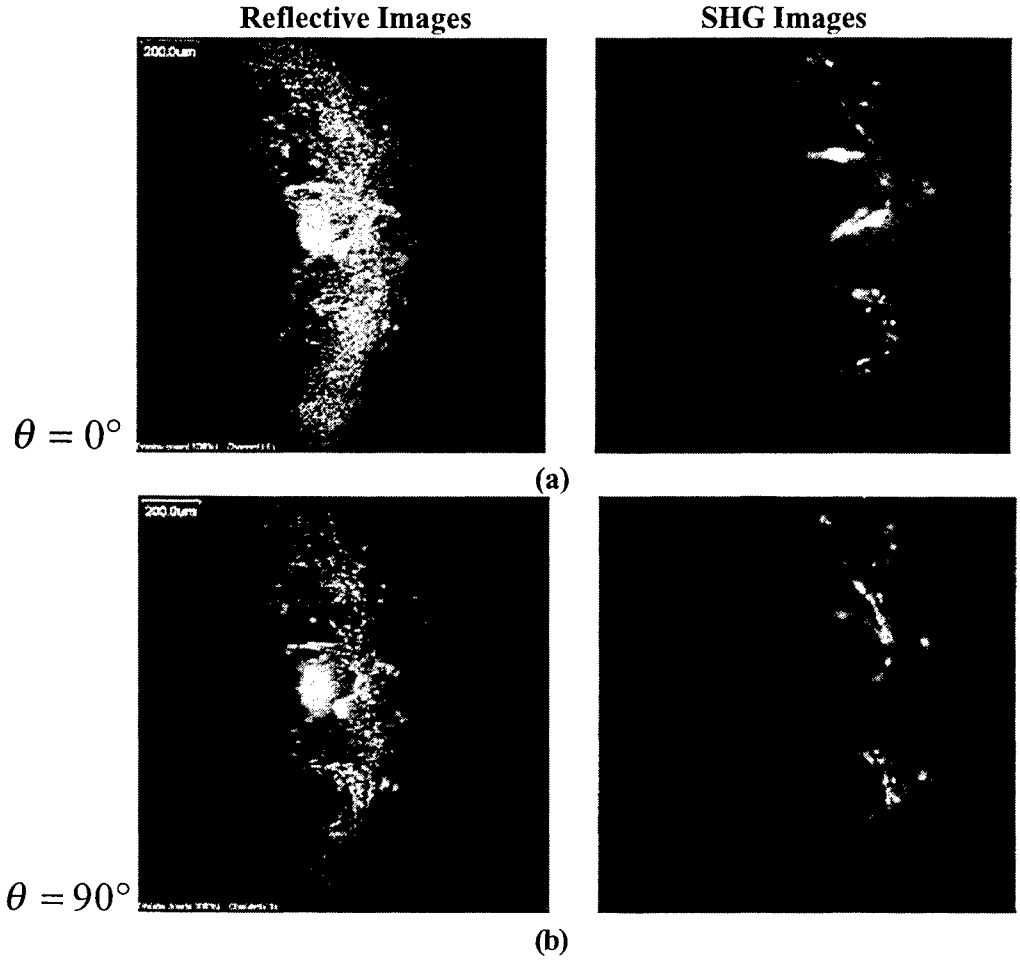

Figure 6. Reflective and SHG images acquired at two different polarization orientations that are perpendicular to each other. The reflective images obtained at the two polarization orientations are basically the same. The big bright spot in the center of reflective images is characteristics to such images, which results from back reflection from lens in the scanning laser beam path. For comparison, the SHG images show very clear contrast. In addition, the different pattern obtained at the two polarization orientations indicates that the tooth is highly anisotropic.

4. DISCUSSION

The theory of surface SHG has been well developed. The physical origin of surface SHG can be attributed to structural discontinuity and field discontinuity at the interface. It was believed that the effect of structural discontinuity dominates a semiconductor surface with dangling bonds. On the other hand, field discontinuity may dominate a liquid or glass surface, where the surface structure is not very different from that in the bulk.[2,3] A surface modification should certainly be distinguishable by surface SHG even in the presence of bulk contribution. Many experiments have shown that surface SHG can reach sub-monolayer sensitivity.[10] From the discussion in the above section, signal intensity in the order of 10^5 photons/sec is attainable, which is sufficient for forming a SHG microscopic image within reasonable time scale. When compared with SHG generated in the bulk that satisfies phase matching conditions, the surface SHG is relatively weak. It is

thus necessary to employ highly sensitive detecting schemes as described above for image acquisition. The maximum SHG intensity available is limited by the onset of surface damages that may result from multi-photon ionization or free electron acceleration heating.

5. CONCLUSIONS

In summary, we have developed a high performance microscopic system for SHG imaging. Using the above system, we have successfully acquired microscopic second-harmonic images of a tooth. Methods of polarization rotation, micro-spectroscopy, and wavelength tuning were also employed to verity the authenticity of the SHG signal. The signal that forms the image contrast is likely the surface SHG from the enamel layer that encapsulating the dentine.

The spatial resolution should be comparable with other two-photon techniques, such as two-photon fluorescence microscopy.[9] We expect that the technique thus developed will find further applications in microscopic inspection of many other systems, such as mineral samples, semiconductor surfaces or interfaces, biological systems, *..etc*. The highly sensitive SHG imaging system described above also has the advantage of being relatively fast in image acquisition. It allows frame rate at 300 seconds/frame with resolution at 512x512 pixels. If a sample is raster-scanned with a 2D translation stage at the same resolution and a PMT is used for signal detection, the frame rate could well exceed hours. Sensitivity and speed will be determining factors for practical applications of the SHG microscopic systems.

ACKNOWLEDGEMENT

We gratefully acknowledge support of this research by the National Science Council of Taiwan under Grant NSC89-2112-M-110-016 and NSC-89-2216-E-110-003 and by the Academic Excellence Program of the Ministry of Education (89-B-FA08-1-4).

REFERENCES

1. A Yariv, *Quantum Electronics 3rd edition,* John Wiley & Sons, New York, 1989.
2. R. Shen, *The Principles of Nonlinear Optics*, John Wiley & Sons, New York, 1984.
3. Y.R. Shen, "Surface properties probed by second-harmonic and sum-frequency generation", *Nature* **337**, pp. 519-525, 1989.
4. J.N. Gannaway and C.J.R. Sheppard, "Second-harmonic imaging in the scanning optical microscope", *Opt. Quantum Electron.* **10**, pp. 435-439, 1978.
5. J. Vydra and M. Eich, "Mapping of the lateral polar orientational distribution in second-order nonlinear thin films by scanning second-harmonic microspectrsocopy", *Appl. Phys. Lett.* **72**, pp. 275-277, 1998
6. R. Gauderon, P.B.Lukins, and C.J.R. Sheppard, "Three-dimensional second-harmonic generation imaging with femtosecond laser pulses", *Opt. Lett.* **23**, pp. 1209-1211, 1998.
7. Y. Guo *et al*, "Optical harmonic generation from animal tissues by the use of picosecond and femtosecond laser pulses", *Appl. Opt.* **35**, pp. 6810-6813, 1996.
8. Y. Guo *et al*, "Second-harmonic tomograpy of tissues", *Opt. Lett* **22**, pp1323-1325, 1997.
9. W. Denk, J.H. Strickler, and W.W. Webb, "Two-Photon Laser Scanning Fluorescence Microscopy", *Science* **248**, pp. 73-76, 1990.
10. T.F Heinz *et al*, "Spectroscopy of molecular monolayers by resonant second-harmonic generation", *Phys. Rev. Lett.* **48**, pp. 478-481, 1982